Acoustic resonances of adsorbed wires and channels

1993 J. Phys.: Condens. Matter 5 8177

(http://iopscience.iop.org/0953-8984/5/44/010)

J. Phys.: Condens. Matter 5 (1993) 8177–8194. Printed in the UK

Acoustic resonances of adsorbed wires and channels

B Djafari-Rouhani and L Dobrzynski

Equipe de Dynamique des Interfaces, Laboratoire de Dynamique et Structure des Matériaux Moléculaires, Unité de Recherche associée au CNRS 801, Unité de Physique, Université de Lille I, F-59655 Villeneuve d'Ascq, France

Received 28 May 1993

Abstract. We present an exact numerical method for obtaining the variation in the density of states associated with the adsorption of wires on a flat surface and with channels cut into an otherwise planar surface. This general method is presented for the determination of the resonances of shear horizontal polarization associated with such surface protuberances or indentations.

1. Introduction

Because of the progress of techniques such as microlithography or molecular beam epitaxy, it is possible to create well defined grooves or adsorbed wires on an otherwise planar surface. The activity around the electronic properties of such quantum wires is in constant expansion. The acoustic resonances of shear horizontal polarization associated with adsorbed wires started to be studied [1] on a simple structure consisting of a rectangular ridge fabricated from a material having a different mass density and elastic moduli from the substrate on which this ridge was adsorbed. The theoretical method used to solve this problem was adapted to the rectangular form of the ridge. A general Green function theory was also proposed [2] for the study of such acoustic resonances localized in the vicinity of an isolated protuberance or indentation on the otherwise planar stress-free surface of a semi-infinite elastic medium. This approach enabled one to calculate the lowest frequencies of acoustic resonances associated with grooves and ridges of the same nature as the substrate.

In the present paper, we show how this Green function approach can be extended to adsorbed wires of different nature from the substrate. We show also how to obtain the variation in the vibrational density of states between the surface with and without the adsorbed wire. Knowledge of this entity gives not only the frequencies of the acoustic resonances localized in the vicinity of the wires but also the width of these resonances.

We shall consider the following systems:

(i) the infinite material;

(ii) the isolated wire (figure 1(a)) limited by two different free surfaces, called respectively M_2 for $-R < x_1 < +R$ and $x_3 = 0$, and M_1 for $x_3 = \xi(x_1)$;

(iii) the semi-infinite substrate (figure 1(b)) limited by the $x_3 = 0$ free surface;

(iv) the same substrate but with a channel having the M_1 ($x_3 = \xi(x_1)$) shape (figure 1(c));

(v) the adsorbed wire (figure 1(d));

(vi) the filled channel (figure 1(e)).

0953-8984/93/448177+18$07.50

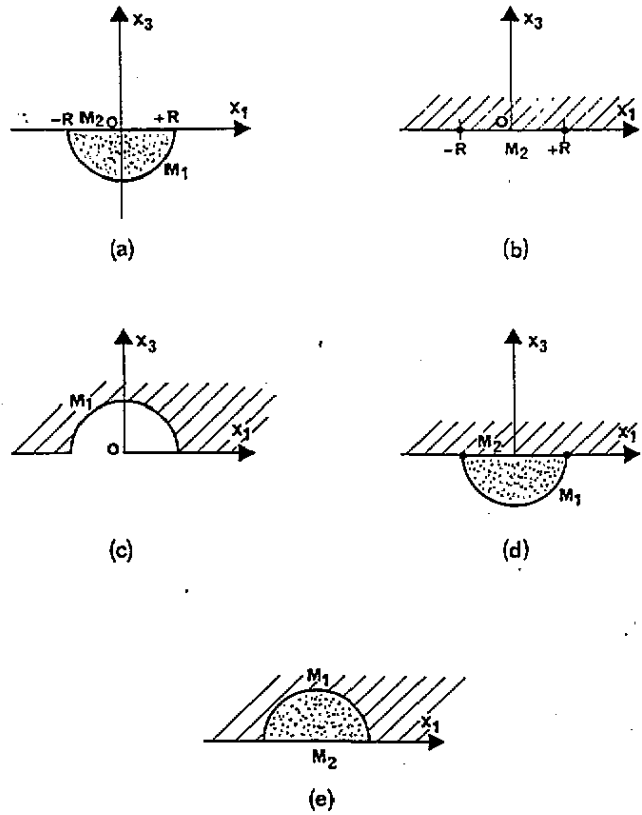

Figure 1. Schematic presentation of the systems studied in this paper: (*a*) the isolated wire; (*b*) the semi-infinite substrate; (*c*) the empty channel; (*d*) the adsorbed wire; (*e*) the filled channel.

We show that the study of the resonances associated with the systems presented in figure 1 involves only the knowledge of the corresponding Green function between points belonging to the M_1 and M_2 surfaces. We shall explain using the example of shear horizontal polarized vibrations how to calculate these Green functions elements out of the bulk Green functions for the isolated wire (figure 1(*a*)) and for the flat surface (figure 1(*b*)).

For the channel (figure 1(*c*)), the Green function between the points lying along M_1 will be obtained from knowledge of the surface Green function of the system in figure 1(*b*). The M_2 interface elements for the adsorbed wire will be obtained from knowledge of the surface Green function along the M_2 free surfaces of the constituent systems in both figure 1(*a*) and figure 1(*b*). In the same manner using the surface Green functions along the M_1 surface of the system in figures 1(*a*) and 1(*c*) we obtain the composite Green function along M_1 for the system in figure 1(*e*).

In the next section, we outline how the above interface elements of the Green functions are obtained in the case of vibrations with polarization parallel to the wires or the channels. Then, in section 3, we derive the general theoretical expressions enabling us to calculate the variation in the density of states between the flat surface (figure 1(*b*)) and each of the three systems depicted in figures 1(*c*), 1(*d*) and 1(*e*). Finally, the method is illustrated by the determination of the resonances associated with adsorbed wires, channels and filled channels of parabolic shape.

2. The interface elements of the Green functions

We assume that the wire and the channel are oriented parallel to the x_2 axis. The elastic displacement field is assumed to have shear horizontal polarization, i.e. to have the form

$$u(x,t) = (0, u_2(x_1, x_3|\omega), 0)\exp(-i\omega t). \tag{1}$$

The bulk equation of motion for vibrations with a propagation vector $k_2 = 0$ can be written as [2]

$$C_{44}(\partial^2/\partial x_1^2 + \partial^2/\partial x_3^2 + \omega^2/c_t^2)u_2(x_1, x_3|\omega) = 0 \tag{2}$$

where C_{44} is the elastic constant and c_t the transverse speed of sound ($c_t = \sqrt{C_{44}/\rho}$ where ρ is the mass density).

We also introduce a Green function $G(x_1, x_3|x_1', x_3')$ for the infinite elastic medium as the solution to the equation

$$C_{44}(\partial^2/\partial x_1^2 + \partial^2/\partial x_3^2 + \omega^2/c_t^2)G(x_1, x_3|x_1', x_3') = \delta(x_1 - x_1')\delta(x_3 - x_3') \tag{3}$$

which satisfies outgoing wave conditions at infinity. A useful representation of this function is

$$G(x_1, x_3|x_1', x_3') = -(i/4C_{44})H_0^{(1)}\{(\omega/c_t)[(x_1 - x_1')^2 + (x_3 - x_3')^2]^{1/2}\} \tag{4}$$

where $H_0^{(1)}(z) = J_0(z) + iY_0(z)$ is a Hankel function of the first kind.

In what follows we shall respectively consider the five systems depicted in figure 1.

2.1. The isolated wire (figure 1(a))

The Green function $g_a(x_1, x_3|x_1', x_3')$ for the isolated wire with stress free surfaces is given also by equation (3) together with the appropriate boundary conditions. In the usual way [2–4], we can obtain an integral equation for $\mathbf{g}_a$ by using the Green theorem and the boundary conditions. For this purpose, we multiply equation (3) for $\mathbf{g}_a$ by $\mathbf{G}$, equation (3) for $\mathbf{G}$ by $\mathbf{g}_a$, subtract and integrate over the whole volume D_a of the wire to obtain

$$g_a(x_1, x_3|x_1', x_3') + \int_{-R}^{+R} dx_1''\, A_a^{(M_1)}(x_1, x_3|x_1'', \xi(x_1''))g_a(x_1'', \xi(x_1'')|x_1', x_3') + \int_{-R}^{+R} dx_1''\, A_a^{(M_2)}(x_1, x_3|x_1'', 0)g_a(x_1'', 0|x_1', x_3') = G(x_1, x_3|x_1', x_3'). \tag{5}$$

The two-dimensional vectors $x = (x_1, x_3)$ and $x' = (x_1', x_3')$ belong to D_a, while the vectors $x'' = (x_1'', \xi(x_1''))$ or $(x_1'', 0)$ run over the boundary curves M_1 and M_2 of the wire, with $M_1 = \{-R < x_1 < R; x_3 = \xi(x_1)\}$ and $M_2 = \{-R < x_1 < R; x_3 = 0\}$. The operators $\mathbf{A}_a^{(M_1)}$ and $\mathbf{A}_a^{(M_2)}$ associated with the M_1 and M_2 curves are defined as

$$A_a^{(M_1)}(x_1, x_3|x_1'', x_3'') = C_{44}[-\xi'(x_1'')\,\partial/\partial x_1'' + \partial/\partial x_3'']G(x_1, x_3|x_1'', x_3'')|_{x_3''=\xi(x_1'')} \tag{6}$$

for $x'' \in M_1$ and

$$A_a^{(M_2)}(x_1, x_3|x_1'', x_3'') = C_{44}(-\partial/\partial x_3'')G(x_1, x_3|x_1'', x_3'')|_{x_3''=0} \tag{7}$$

for $x'' \in M_2$.

Instead of equation (5) for $\mathbf{g}_a(D_a, D_a)$, we can first limit ourselves to an integral equation for $\mathbf{g}_a(M, M)$ only, with $M \equiv \{M_1, M_2\}$. In this case, we have to set $x_3 = \xi(x_1) + \epsilon$ on M_1 and $x_3 = -\epsilon$ on M_2, with ϵ an infinitesimal number. In order to solve numerically this integral equation, we have to transform it into a discrete matrix equation. For this purpose, we introduce along the x_1 axis a set of $2N$ equally spaced points $\{x_n\}$ such that

$$x_n = (n + \tfrac{1}{2})\,\Delta x \qquad \text{with } n = -N, -N+1, \ldots, N-1 \text{ and } \Delta x = R/N. \tag{8}$$

In this way, the curves M_1 and M_2 are divided into small portions which can be labelled as (x_n, i) where $i = 1, 2$ stands for M_1 or M_2. Then, we integrate both members of the integral equation over the variable x_1' inside the elementary interval associated with the point (x_m, i). We obtain the following discrete equation:

$$g_a(ni|mj) + \sum_{k=1}^{2} \sum_{l=-N}^{N-1} A_a(ni|lk) g_a(lk|mj) = G(ni|mj). \tag{9}$$

In this equation, the discrete elements of the operators $\mathbf{G}$, $\mathbf{g}_a$ and $\mathbf{A}_a$ are given by their average values over each interval in the following way. The discrete elements of the bulk Green function will be defined as follows.

(i) For $x' \in M_1$,

$$G(ni|m1) = \frac{1}{\Delta x} \int_{x_m - \Delta x/2}^{x_m + \Delta x/2} \mathrm{d}x_1' \,\{1 + [\xi'(x_1')]^2\}^{1/2} G(x_n, i; x_1', 1). \tag{10a}$$

(ii) For $x' \in M_2$,

$$G(ni|m2) = \frac{1}{\Delta x} \int_{x_m - \Delta x/2}^{x_m + \Delta x/2} \mathrm{d}x_1' \, G(x_n, i; x_1', 2). \tag{10b}$$

Similar equations hold for the elements of $\mathbf{g}_a$ and also of $\mathbf{A}_a$ except, in the case of the latter operator, for the factor Δx appearing in front of the integrals in equations (10).

Let us define the matrix $\mathbf{\Delta}_a(MM)$ whose elements between all the points of the surface space M are

$$\Delta_a(ni|mj) = \delta_{nm}\delta_{ij} + A_a(ni|mj) \tag{11}$$

and the matrices $\mathbf{G}(MM)$ and $\mathbf{g}_a(MM)$ whose elements are respectively $G(ni|mj)$ and $g_a(ni|mj)$. With this notation, equation (9) reads

$$\mathbf{g}_a(MM)\mathbf{\Delta}_a(MM) = \mathbf{G}(MM). \tag{12}$$

The matrix elements of $\mathbf{G}(MM)$ and $\mathbf{\Delta}_a(MM)$ can be evaluated analytically to first order in Δx. Their values are given in the appendix. By straightforward matrix algebra, we can now obtain from equation (12), the matrix $\mathbf{g}_a(MM)$, and in particular its truncated part $\mathbf{g}_a(M_iM_i)$ ($i = 1$ or 2) for the points situated along the surfaces M_1 or M_2, respectively. We shall see in what follows that we shall need the inverse $[\mathbf{g}_a(M_2M_2)]^{-1}$ of this truncated part for the study of the adsorbed wire (figure 1(*e*)).

The eigenfrequencies of the isolated wire are interesting by themselves. They can be obtained from the poles of any element of the matrix $\mathbf{g}_a$ and in particular from

$$\det[\mathbf{g}_a(M_iM_i)]^{-1} = 0 \qquad i = 1 \text{ or } 2. \tag{13}$$

Because the wire is finite in the $(\hat{x}_1, \hat{x}_3)$ plane, the eigenfrequencies of the wire, for $k_2 = 0$, are discrete and there is an infinite number of them.

2.2. The semi-infinite substrate with a planar surface (figure 1(b))

Let us now consider the semi-infinite medium such that $x_3 \geqslant 0$, with the stress-free surface at $x_3 = 0$.

The Green function associated with this system is well known [3] to be

$$g_b(x_1, x_3|x_1', x_3') = -(i/4C_{44})H_0^{(1)}\{(\omega/c_t)[(x_1 - x_1')^2 + (x_3 - x_3')^2]^{1/2}\} - (i/4C_{44})H_0^{(1)}\{(\omega/c_t)[(x_1 - x_1')^2 + (x_3 + x_3')^2]^{1/2}\}. \quad (14)$$

In what follows, we shall need only the matrix elements of this Green function $\mathbf{g}_b$ between the $2N$ discrete points defined above along the M_2 surface ($-R \leqslant x_1 \leqslant +R$). These matrix elements are calculated also by integration over the interval Δx, in the same manner as above for the bulk Green function $\mathbf{G}$. Their explicit values are given in section A2 of the appendix.

2.3. The channel (figure 1(c))

The channel will be constructed by cutting out the wire (figure 1(*a*)) from the semi-infinite material (figure 1(*b*)). This can be done in a manner similar to what we did before for the wire, in section 2.1, but now we use the surface Green function $\mathbf{g}_b$ instead of the bulk Green function $\mathbf{G}$ and obtain, instead of equation (5),

$$g_c(x_1, x_3|x_1', x_3') + \int_{-R}^{+R} dx_1'' \, A_c(x_1, x_3|x_1'', -\xi(x_1''))g_c(x_1'', -\xi(x_1'')|x_1', x_3') = g_b(x_1, x_3|x_1', x_3'). \quad (15)$$

We take the shape of the channel, the form $x_3 = -\xi(x_1)$, where $\xi(x_1)$ has the same expression as for the wire in section 2.1. Then

$$A_c(x_1, x_3|x_1'', -\xi(x_1'')) = C_{44}(\xi'(x_1'')\,\partial/\partial x_1'' + \partial/\partial x_3'')g_b(x_1, x_3|x_1'', x_3'')|_{x_3''=-\xi(x_1'')}. \quad (16)$$

Following then the same procedure as in section 2.1, we end up with the following matrix equation:

$$\mathbf{g}_c(M_i M_1)\boldsymbol{\Delta}_c(M_1 M_1) = \mathbf{g}_b(M_i M_1). \quad (17)$$

The matrix elements of $\mathbf{g}_b(M_1 M_i)$ and $\boldsymbol{\Delta}_c(M_1 M_1)$ are given in section A3 of the appendix.

It should be noted that the same procedure also gives the matrix elements along the M_1 surface of the Green function $\mathbf{g}_w(M_1 M_1)$ of the isolated wire complementary to the channel in figure 1(*c*). When using this approach, one must remember that the derivative along the normal to the surface changes its sign compared with the channel calculation. Then, we obtain

$$\mathbf{g}_w(M_i M_1)\boldsymbol{\Delta}_w(M_i M_1) = \mathbf{g}_b(M_i M_1) \quad (18)$$

where the matrix elements of $\mathbf{g}_b(M_i M_1)$ are the same as those for the channel (equations (A16)–(A17)) and those of $\boldsymbol{\Delta}_w(M_i M_1)$ are given in section A3 of the appendix. Of course,

$$\mathbf{g}_w(M_i M_1) \equiv \mathbf{g}_a(M_i M_1). \quad (19)$$

2.4. The adsorbed wire (figure 1(d))

For the adsorbed wire, we can also use the Green theorem in the usual manner [2–4], but with the surface Green functions $\mathbf{g}_a$ and $\mathbf{g}_b$ rather than the corresponding bulk Green functions $\mathbf{G}_a$ and $\mathbf{G}_b$. Now the indices a and b refer in general to respectively an isolated wire and a substrate having different mass densities and elastic moduli. The Green function for the adsorbed wire will be denoted $\mathbf{g}_d$.

We multiply equation (3) for $\mathbf{g}_d$ by $\mathbf{g}_a$, equation (3) for $\mathbf{g}_a$ by $\mathbf{g}_d$, subtract and integrate over the whole volume of the adsorbed wire using the Green theorem and the stress-free boundary conditions to obtain for (x_1, x_3) and (x_1', x_3') both inside the wire

$$g_d(x_1, x_3|x_1', x_3') - g_a(x_1, x_3|x_1', x_3') = -\int_{-R}^{+R} dx_1''\, g_a(x_1, x_3|x_1'', x_3'' = 0)\left(C_{44}^{(a)}\frac{\partial}{\partial x_3''}[g_d(x_1'', x_3''|x_1', x_3')]\Big|_{x_3''=0}\right). \quad (20)$$

When (x_1, x_3) is inside the substrate and (x_1', x_3') is inside the wire, we obtain in the same way

$$g_d(x_1, x_3|x_1', x_3') = \int_{-R}^{+R} dx_1''\, g_b(x_1, x_3|x_1'', x_3'' = 0)\left(C_{44}^{(b)}\frac{\partial}{\partial x_3''}[g_d(x_1'', x_3''|x_1', x_3')]\Big|_{x_3''=0}\right). \quad (21)$$

We use the requirement of the continuity of the stresses across the flat interface M_2 and discretize the equations (20) and (21) in the same manner as above. Eliminating the derivative of $\mathbf{g}_d$ between these two equations [4], we obtain the following useful relation:

$$[\mathbf{g}_d(M_2M_2)]^{-1} = [\mathbf{g}_a(M_2M_2)]^{-1} + [\mathbf{g}_b(M_2M_2)]^{-1} \quad (22)$$

which ensures that the displacements and the stresses are continuous across the interface M_2.

2.5. The filled channel (figure 1(e))

For the filled channel, it is straightforward to repeat the demonstration done above for the adsorbed wire and to obtain its interface elements $\mathbf{g}_e(M_1M_1)$ from those of the empty channel and those of the wire, through the following relations:

$$[\mathbf{g}_e(M_1M_1)]^{-1} = [\mathbf{g}_c(M_1M_1)]^{-1} + [\mathbf{g}_w(M_1M_1)]^{-1}. \quad (23)$$

As outlined in the next section, the above interface elements of the Green functions corresponding to all the systems considered in this paper are sufficient for the studies of the variation, compared with the flat substrate, in the densities of states.

3. Densities of states and resonances

The local density of states per unit of ω for a given system can be obtained from its Green function $\mathbf{g}$ by the standard formula

$$n(x_1, x_3, \omega) = -\lim_{\epsilon\to 0}\{[2\rho(x_1, x_3)\omega/\pi]\,\mathrm{Im}[g(x_1, x_3; x_1, x_3|\omega + i\epsilon)]\} \quad (24)$$

where $\rho(x_1, x_3)$ is the mass density at the local point (x_1, x_3). The factor $2\rho(x_1, x_3)\omega$ appears because of the definition used here for the Green functions (see equation (3)).

The total density of states can be obtained in the same manner:

$$n(\omega) = -\lim_{\epsilon \to 0}[[(2\omega/\pi)\,\mathrm{Tr}\{\rho(x_1, x_3)\,\mathrm{Im}[g(x_1, x_3; x_1, x_3|\omega + \mathrm{i}\epsilon)]\}]]. \tag{25}$$

Before going into the evaluation of the trace appearing in equation (25), let us recall how a Green function for a composite made out of two different materials can be calculated between any two different points of the composite. Although the following demonstration is completely general, we shall outline it using the example of the adsorbed wire. The starting point is equations (20) and (21) and the similar equations that one can obtain when (x_1', x_3') is inside the substrate and (x_1, x_3) is first in the substrate and then in the wire. These four equations are then discretized as explained above, in order to transform them into matrix equations. This enables us then to obtain different relations between the reference Green functions $\mathbf{g}_a$ and $\mathbf{g}_b$ and the composite Green function $\mathbf{g}_d$. The relation [5] of interest here will be written with the following general matrix notations:

$$\mathbf{g}_s(DD) = \begin{bmatrix} \mathbf{g}_a(D_aD_a) & \mathbf{0} \\ \mathbf{0} & \mathbf{g}_b(D_bD_b) \end{bmatrix} \tag{26}$$

where D is the whole discretized space of the adsorbed wire, D_b its substrate part and D_a its wire part. The discrete points near the M_2 interface are at $x_3 = -\epsilon$ in D_a and at $x_3 = +\epsilon$ in D_b. So $\mathbf{g}_s(DD)$ is a matrix formed out of two disconnected blocks.

Using the same notation for $\mathbf{g}_d$, one obtains the matrix equation

$$\mathbf{g}_d(DD) = \mathbf{g}_s(DD) - \mathbf{g}_s(DM_2)[\mathbf{g}_s(M_2M_2)]^{-1}\mathbf{g}_s(M_2D) + \mathbf{g}_d(DM_2)[\mathbf{g}_d(M_2M_2)]^{-1}\mathbf{g}_d(M_2D). \tag{27}$$

$\mathbf{g}_s$ and $\mathbf{g}_d$ are complete (and not truncated) matrices. For such complete and diagonalizable matrices we utilize the cyclic invariance of the trace and the two following general properties:

$$\mathbf{g}(MD)\mathbf{g}(DM) = -\mathrm{d}\mathbf{g}(MM)/\mathrm{d}(\rho\omega^2) \tag{28}$$

and

$$\mathrm{Tr}\{[\mathbf{g}(MM)]^{-1}\,\mathrm{d}\mathbf{g}(MM)/\mathrm{d}(\rho\omega^2)\} = \mathrm{d}[[\ln\{\det[\mathbf{g}(MM)]\}]]/\mathrm{d}(\rho\omega^2). \tag{29}$$

Together with equations (25)–(27) they enable us to obtain for the variation in the density of states between the adsorbed wire on the one hand (figure 1(d)) and the uncoupled substrate (figure 1(b)) and isolated wire (figure 1(a)) on the other hand the following result:

$$n_d(\omega) - n_b(\omega) - n_a(\omega) = (1/\pi)(\mathrm{d}/\mathrm{d}\omega)[[\arg\{\det[\mathbf{g}_d(M_2M_2)/\mathbf{g}_a(M_2M_2)\mathbf{g}_b(M_2M_2)]\}]] \tag{30}$$

where $\mathbf{g}_d(M_2M_2)$ can be expressed as a function of $\mathbf{g}_a(M_2M_2)$ and $\mathbf{g}_b(M_2M_2)$ through the relation (22). This enables us to express equation (30) in the following equivalent forms:

$$n_d(\omega) - n_b(\omega) - n_a(\omega) = (1/\pi)(\mathrm{d}/\mathrm{d}\omega)[[\arg\{\det[\mathbf{g}_a(M_2M_2) + \mathbf{g}_b(M_2M_2)] \tag{31a}$$

or

$$n_d(\omega) - n_b(\omega) - n_a(\omega) = (1/\pi)(d/d\omega)(\arg[\![\det\{[\mathbf{g}_a(M_2M_2)]^{-1} + [\mathbf{g}_b(M_2M_2)]^{-1}\}]\!] - \arg[\![\det\{[\mathbf{g}_a(M_2M_2)]^{-1}\}]\!] - \arg[\![\det\{[\mathbf{g}_b(M_2M_2)]^{-1}\}]\!]). \quad (31b)$$

In fact, we are interested by the variation $\Delta n(\omega) = n_d(\omega) - n_b(\omega)$ in the density of states due to the deposition of the wire onto the flat surface of the substrate. This will be given by the right-hand side (RHS) of equation (31*b*) in which the delta peaks associated with the eigenfrequencies of the isolated wire (solutions of $\det[\mathbf{g}_a(M_2M_2)]^{-1} = 0$) are eliminated. Choosing to disregard the discrete delta peaks, we can also obtain $\Delta n(\omega)$ through the expression

$$(1/\pi)(d/d\omega)(\arg[\![\det\{[\mathbf{g}_a(M_2M_2)]^{-1} + [\mathbf{g}_b(M_2M_2)]^{-1}\}]\!] - \arg\{\det[\mathbf{g}_b(M_2M_2)]^{-1}\}). \quad (31c)$$

Indeed, let us first note that, owing to the finiteness of the isolated wire, the quantity $\arg\{\det[\mathbf{g}_a(M_2M_2)]^{-1}\}$ is always equal to 0 modulo π. In comparison with the RHS of equation (31*b*), we have eliminated in equation (31*c*) the delta peaks associated with the solutions of $\det[\mathbf{g}_a(M_2M_2)]^{-1} = 0$. However, we have introduced new delta functions connected to the solutions of $\det[\mathbf{g}_a(M_2M_2)] = 0$ (see discussion of equation (32*b*) below) which did not exist in the RHS of equation (31*b*) owing to compensation between the first two terms.

In the practice of the numerical calculations, we have used both equation (31*b*) and equation (31*c*) to evaluate $\Delta n(\omega)$ disregarding in each case the peaks representing delta functions. In view of the discussion of these numerical applications presented in section 4, let us now consider two limiting cases of equations (31). First, when the elastic constant $C_{44}^{(b)}$ of the substrate becomes vanishingly small, the elements of the matrix $[\mathbf{g}_b(M_2M_2)]^{-1}$ go to zero and so does the RHS of equation (31*b*). The physical meaning of this result is that the eigenmodes of the isolated wire, with stress-free boundary conditions, are not perturbed by the substrate and, therefore, we have the situation of a wire surrounded by vacuum.

In the second limiting case, assume that $C_{44}^{(b)}$ goes to ∞; then the elements of the matrix $\mathbf{g}_b(M_2, M_2)$ become vanishingly small and the RHS of equation (31*a*) reduces to

$$(1/\pi)(d/d\omega)\arg\{\det[\mathbf{g}_a(M_2M_2)]\}. \quad (32a)$$

Physically, in this limit, the planar surface (M_2) of the wire which is in contact with the substrate becomes rigidly bound, whereas its curved surface (M_1) still remains free of stress; in the following, we shall refer to this case as mixed boundary conditions. Therefore, the expression given in equation (32*a*) corresponds to the difference between the densities of states of two isolated wires submitted to mixed and stress free boundary conditions, respectively. One consequence of this analysis is that the eigenfrequencies of the former wire are solutions of

$$\det[\mathbf{g}_a(M_2M_2)] = 0. \quad (32b)$$

A similar result can be derived from the mathematical analysis of [4].

4. Illustrations of acoustic shape resonances

In this section we present and comment on a few calculations of the density of states and shape resonances associated with adsorbed wires and channels. In these applications, the wire (or channel) is limited partly by a planar surface and partly by a curved surface of parabolic shape; this means that the function $\xi(x_1)$ is defined as $\xi(x_1) = -A[1 - (x_1/R)^2]$ for $x_1 \in [-R, R]$; in the following examples we have taken $A = 2R$. In the discretization of the integral equations, the interval $[-R, R]$ is divided into $2N$ equal parts. Owing to the symmetry of the parabola, the acoustic resonances may be distinguished according to their symmetric or antisymmetric character; this enables one to handle matrices of order N (instead of $2N$) for each symmetry. In most of the following calculations, N is put equal to 100.

Let us first give the first few discrete eigenfrequencies of an isolated wire. When the whole surface of the wire is free of stress, these frequencies are obtained as solutions of $\det[\mathbf{g}_a(M_2M_2)]^{-1} = 0$ (equations (13) or (32a)) and become

$$\omega R/c_t = 1.70-3.20-3.65-4.75-5.10-6.15-6.45-6.95-7.60-7.85\ldots$$

for the symmetric modes and

$$1.90 - 3.25 - 4.55 - 5.30 - 5.90 - 6.85 - 7.25\ldots$$

for the antisymmetric modes.

On the other hand, when the planar surface M_2 of the wire is assumed to be rigidly bound whereas its curved surface M_1 is free of stress (mixed boundary conditions), the eigenfrequencies are solutions of $\det[\mathbf{g}_a(M_2M_2)] = 0$ and the first few resonances are given by

$$\omega R/c_t = 0.95 - 2.50 - 3.95 - 4.45 - 5.45 - 5.80$$

for the symmetric modes and

$$2.65 - 3.95 - 6.15 - 6.60$$

for the antisymmetric modes.

Figures 2–4 give the variation $\Delta n(\omega) = n_d(\omega) - n_b(\omega)$ in the total density of states due to the deposition of a wire of material a onto the planar surface of a substrate made of material b. As a comparison, we have also displayed in each figure the local density of states integrated over the (planar) interface between the wire and the substrate. In these few examples the two materials have the same mass densities ($\rho^{(a)}/\rho^{(b)} = 1$) but different elastic constants such that $C_{44}^{(a)}/C_{44}^{(b)} = 1$, 4 and 0.25 in figures 2, 3 and 4, respectively. When the substrate is softer than the wire (figure 3) and even of the same nature (figure 2), there is rather good correspondence between the peaks of the density of states and the discrete eigenfrequencies of the isolated wire with stress-free surfaces; this connection becomes more particularly pronounced when the ratio $C_{44}^{(a)}/C_{44}^{(b)}$ increases. Also, there is a low-frequency resonance of symmetric character which may originate from the static ($\omega = 0$) mode of the isolated wire. One can also see an increase in the background of the density of states as a function of $\omega R/c_t$. Indeed, by increasing ω, or equivalently the lateral size of the wire, we should recover the density of states of a two-dimensional object (remember that the wavevector k_2 parallel to the wire is taken to be zero) which behaves like ω. Now, in

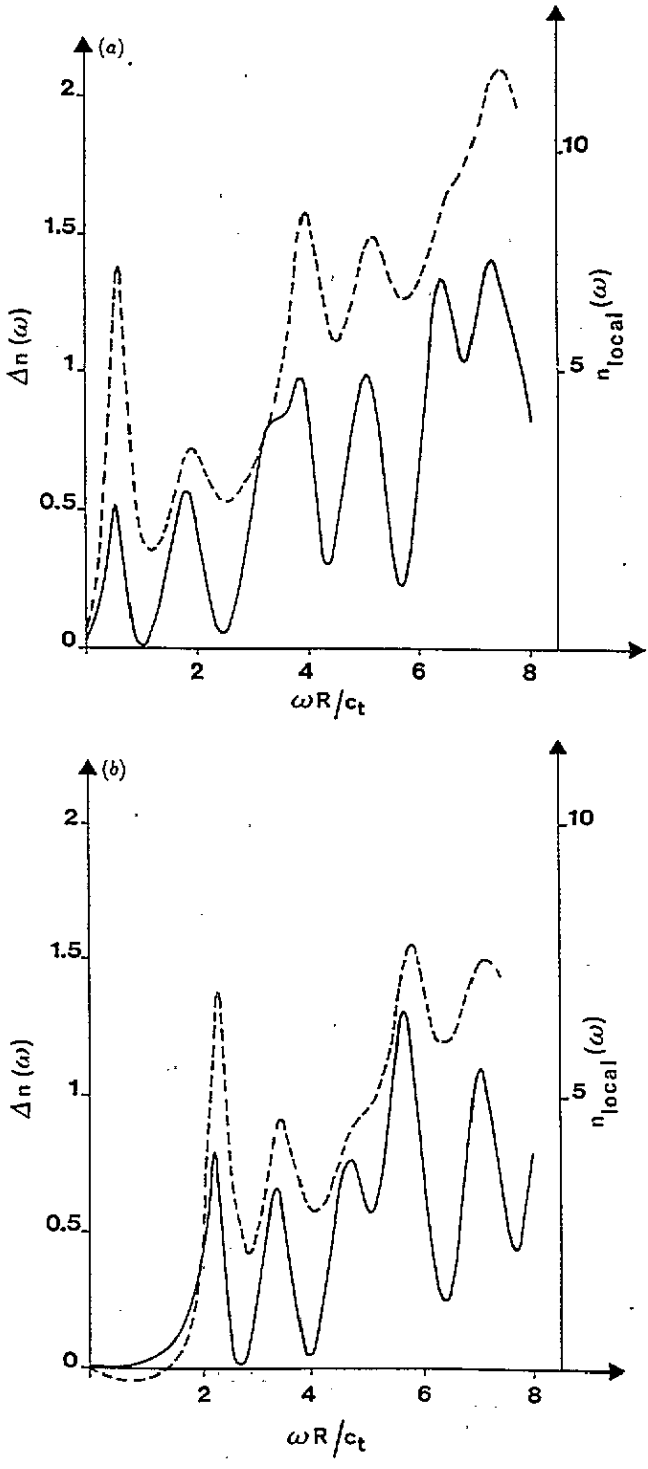

Figure 2. (*a*) Symmetric modes associated with an adsorbed wire of the same material as the substrate: ----, variation in the total density of states (in units of R/c_t) as a function of $\omega R/c_t$; ——, local density of states (in units of $(4c_t)^{-1}$) integrated along the planar interface between the wire and the substrate. (*b*) Same as for (*a*) but for the antisymmetric modes.

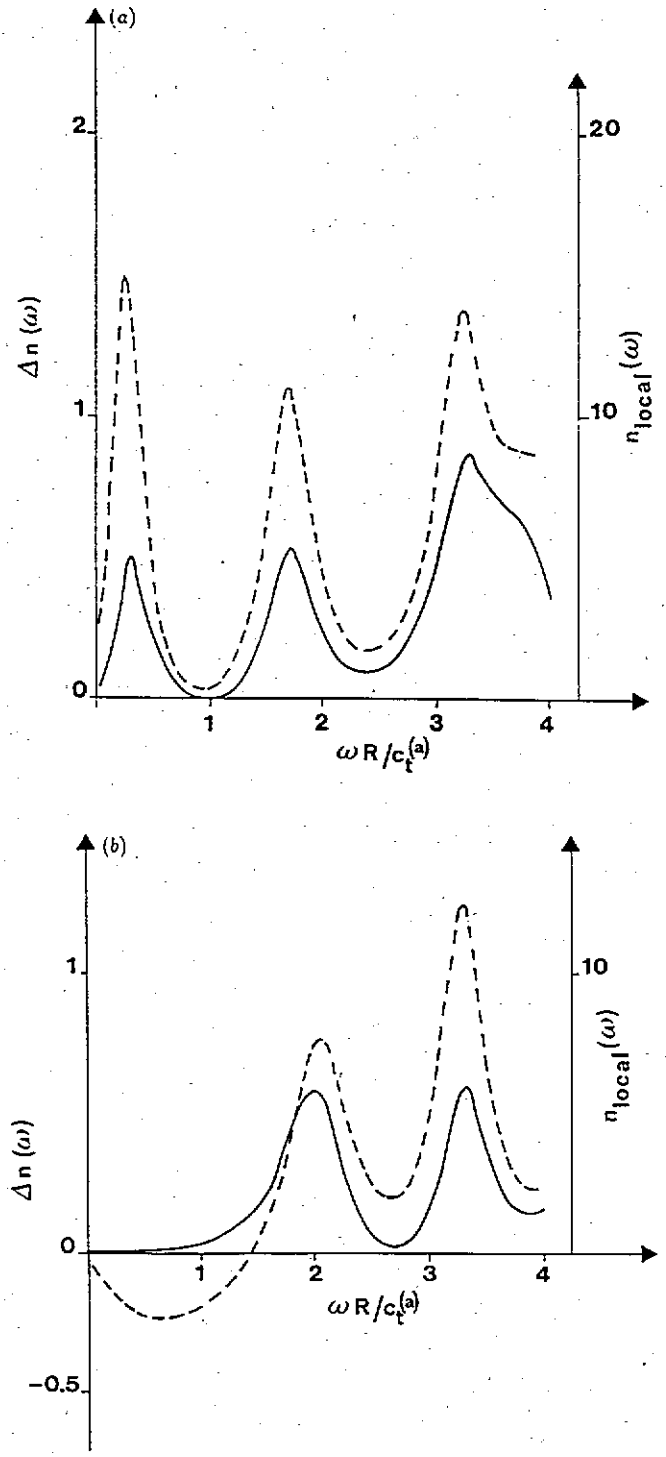

Figure 3. (*a*), (*b*) Same as for figures 2(*a*) and 2(*b*), respectively, but for an adsorbed wire a on a substrate b such that $C_{44}^{(a)}/C_{44}^{(b)} = 4$ and $\rho_{\pm}^{(a)}/\rho^{(b)} = 1$. The quantities reported on both axes are scaled with the velocity of sound in material a.

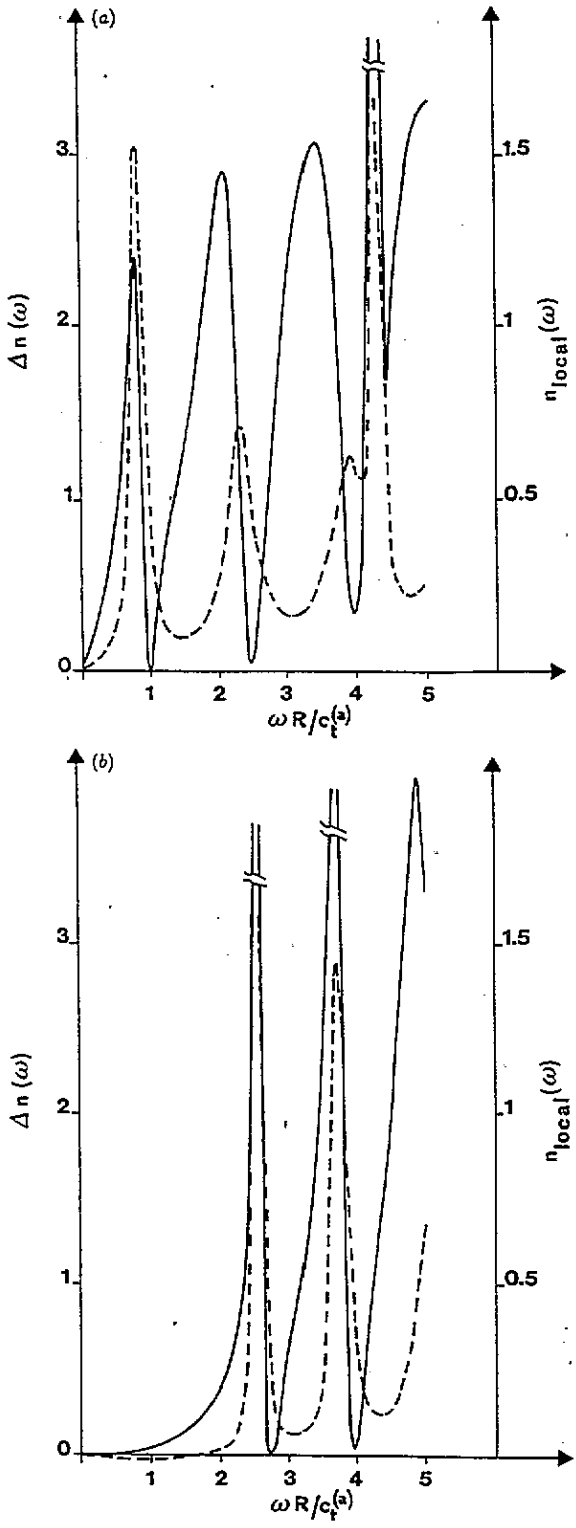

Figure 4. (*a*), (*b*) Same as for figures 3(*a*) and 3(*b*), respectively, but for $C_{44}^{(a)}/C_{44}^{(b)} = 0.25$ and $\rho^{(a)}/\rho^{(b)} = 1$.

our third example in which the wire becomes softer than the substrate (figure 4), one can establish a connection between the peaks in the variation in the total density of states and the eigenfrequencies of the isolated wire with mixed boundary conditions. However, the local density of states over the wire–substrate interface may show a different behaviour in this case.

It is worthwhile making a few technical comments about the numerical calculations. The value $N = 100$ used in our discretization procedure is quite sufficient to obtain with good accuracy the eigenmodes of the isolated wire, as well as the local density of states at the wire–substrate interface. The variation $\Delta n(\omega)$ in the total density of states, derived from either equation (31*b*) or equation (31*c*), is also obtained accurately, except sometimes in the near vicinity of the eigenfrequencies of the isolated wire, with either stress-free or mixed boundary conditions, i.e. when

$$\det[\mathbf{g}_a(M_2M_2)]^{-1} = 0 \tag{33a}$$

or

$$\det[\mathbf{g}_a(M_2M_2)] = 0. \tag{33b}$$

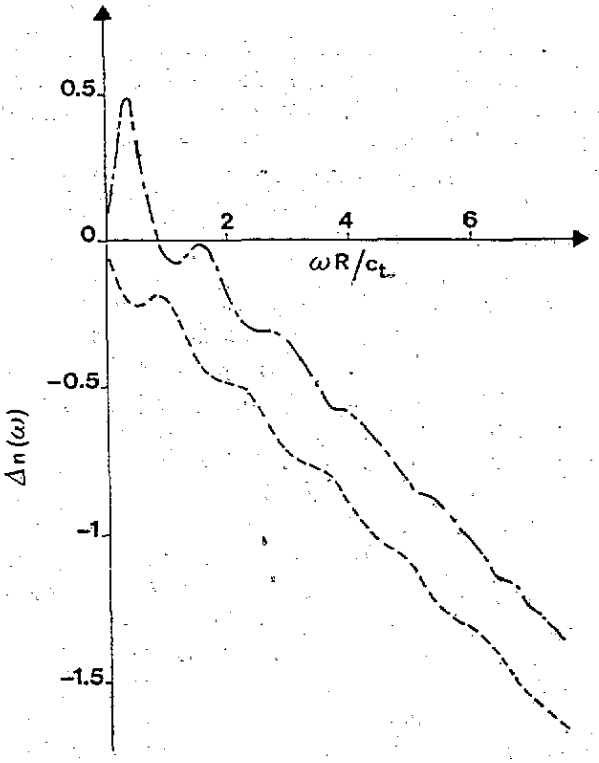

Figure 5. Variation in the total density of states (in units of c_t/R) between a substrate with an empty channel and a flat substrate: ----, symmetric modes; — · —, antisymmetric modes.

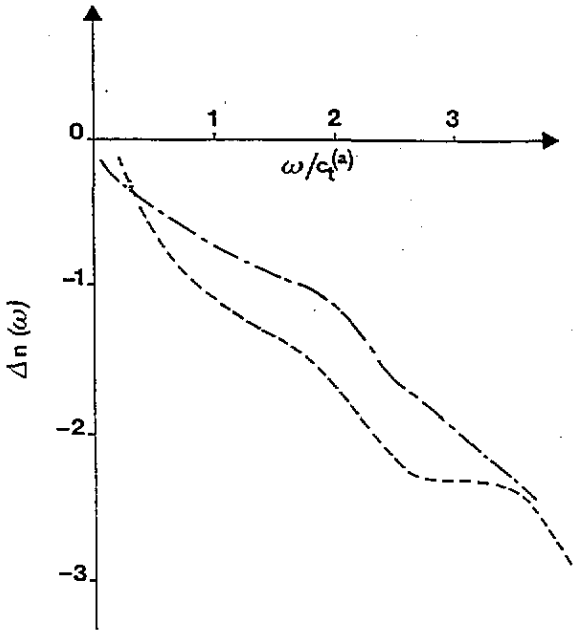

Figure 6. Variation in the total density of states (in units of $c_t^{(a)}/R$) for a channel filled with a material a such that $C_{44}^{(a)}/C_{44}^{(b)} = 4$ and $\rho^{(a)}/\rho^{(b)} = 1$.

Equation (31*b*) may lead to an irregular behaviour in $\Delta n(\omega)$ when ω is near a solution of equation (33*a*), and so does equation (31*c*) near a solution of equation (33*b*). Therefore, in practice, one can evaluate $\Delta n(\omega)$ alternatively from equation (31*b*) or equation (31*c*) when ω is near a solution of equation (33*a*) or of equation (33*b*). However, let us justify the choice of this method by explaining the origin of these artefacts which otherwise decrease very slowly by increasing N (in our calculation we used up to $N = 300$ to overcome only partly these anomalies). Indeed, owing to the discreteness of the isolated wire eigenfrequencies, the quantity $\arg\{\det[\mathbf{g}_a(M_2M_2)]^{-1}\}$ in equation (31*b*) should, in principle, always take the value 0 modulo π. In fact, because of the discretization of the integral equations, this statement is only approximately satisfied and, in particular, requires a very high value of N near the solutions of equations (33). Therefore we can eliminate the corresponding anomalies in the density of states by using alternatively equation (31*b*) and equation (31*c*). Let us emphasize that, far from the eigenmodes of the isolated wire, both equation (31*b*) and equation (31*c*) give similar results and can be used indifferently.

Finally, we give a few examples of the densities of states related to the geometry of a channel or filled channel of parabolic shape near the planar surface of a substrate (figure 1(*c*)). Figure 5 displays the variation in the total density of states, of symmetric or antisymmetric character, when a channel is cut near the planar surface: $\Delta n(\omega) = n_c(\omega) - n_b(\omega)$. The decrease in the background in the density of states can be related to the lack of matter in the new substrate when creating the channel. The most prominent feature in this figure is a low-frequency antisymmetric resonance; also, one can observe a few weak peaks and shoulders. In figures 6 and 7, we have presented the variation in the total density of states when a channel is cut near the planar surface of a substrate b and filled with a different material a: $\Delta n(\omega) = n_e(\omega) - n_b(\omega)$. In these figures, the materials a and b have the same mass densities but different elastic constants such that $C_{44}^{(a)}/C_{44}^{(b)} = 4$

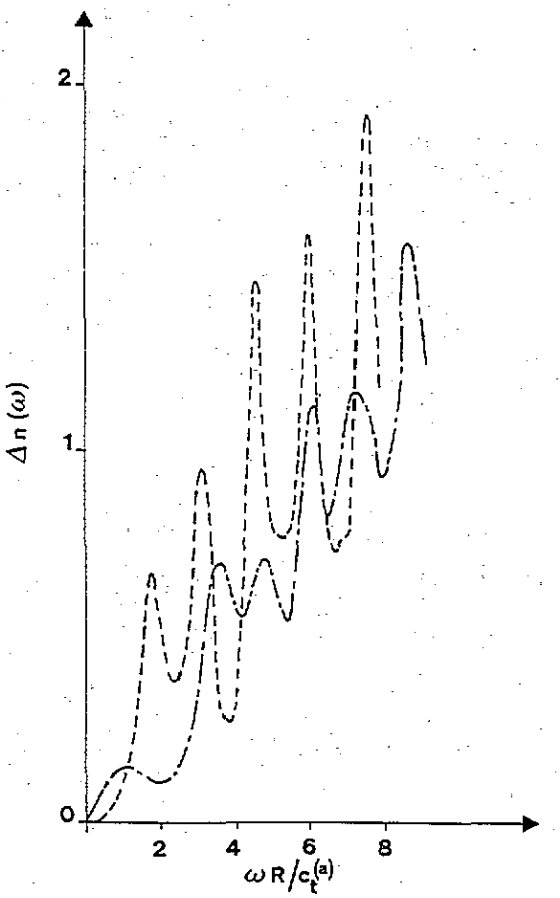

Figure 7. Same as for figure 6 but for $C_{44}^{(a)}/C_{44}^{(b)} = 0.25$ and $\rho^{(a)}/\rho^{(b)} = 1$.

and 0.25, respectively. In figure 6, there are only very broad features but a decrease in $\Delta n(\omega)$ versus ω which can be explained by the higher stiffness of material a compared with the substrate. On the contrary, figure 7 displays an increasing background of $\Delta n(\omega)$ as well as rather sharp peaks. In the limit of a very large ratio $C_{44}^{(b)}/C_{44}^{(a)}$, one should find the eigenmodes of an isolated wire having its planar surface (M_2) free of stress and its curved surface (M_1) rigidly bound. The first few resonances of such a wire are given by $\omega R/c_t = 2.10 - 3.45 - 4.85 - 5.35 - 6.30 - 6.90 - 7.75\ldots$ for symmetric modes and $3.7 - 5.15 - 6.50 - 7.0 - 7.85\ldots$ for antisymmetric modes. The peaks in figure 6 show some similarity with this picture even though the correspondence is not totally satisfactory; higher values of $C_{44}^{(a)}$ might be necessary to achieve good correspondence.

A more detailed analysis of the resonances associated with adsorbed wires and channels will need also the consideration of other shapes or configurations of the wires.

5. Conclusions

We presented in this paper a general method for the calculation of the density of states associated with the adsorption of wires on a flat surface and with empty and filled channels

cut into an otherwise planar surface and illustrated it by a few applications. This method, although outlined for vibrations of shear horizontal polarization, is completely general [6] and will be used for vibrations polarized in the saggital plane. Of course the bulk Green functions may have in general to be calculated numerically. This method should also be useful for the study of other excitations (electrons, magnons and polaritons) in any composite material and in particular in quantum wires and dots.

This method enables us also to address the problems of scattering [6] by wires, channels and dots. Such problems are of current interest for in particular the scattering of acoustic waves by single resonating elements [7–9] and by periodic and quasi-periodic corrugated solid surfaces (see, e.g., [10, 11]). In particular, a correlation was found recently [11] between the resonant frequencies of an adsorbed block and the appearance of a frequency gap in the transmission of ultrasonic waves through a plate decorated with Lucite blocks.

Appendix. Interface matrix elements for the systems studied in this paper

We use the following notation to give the interface matrix elements:

$$\xi(m) = \xi(x_m) \qquad \xi'(m) = [\partial\xi(x_1)/\partial x_1]|_{x_1=x_m} \qquad \xi''(m) = [\partial^2\xi(x_1)/\partial x_1^2]|_{x_1=x_m}$$

and $\log\gamma = 0.577\,215\,664\,9\ldots$ (the Euler number).

A1. The wire (figure 1(a))

The surface elements of the bulk Green function **G** as defined by equations (10) are as follows.

(i) Between two points lying on the M_1 surface,

$$G(n1|m1) = -(\mathrm{i}/4C_{44})\{1+[\xi'(m)]^2\}^{1/2} \times H_0^{(1)}[\![(\omega/c_t)\{(x_n-x_m)^2+[\xi(n)-\xi(m)]^2\}^{1/2}]\!] \qquad n\neq m \tag{A1}$$

$$G(n1|n1) = -(1/4\pi C_{44})\{1+[\xi'(n)]^2\}^{1/2} \times (\mathrm{i}\pi + 2 - 2\log[\![\tfrac{1}{4}\gamma\,\Delta x\,(\omega/c_t)\{1+[\xi'(n)]^2\}^{1/2}]\!]). \tag{A2}$$

(ii) Between two points lying on the M_2 surface,

$$G(n2|m2) = -(\mathrm{i}/4C_{44})H_0^{(1)}[(\omega/c_t)|x_n-x_m|] \qquad n\neq m \tag{A3}$$

$$G(n2|n2) = -(1/4\pi C_{44})\{\mathrm{i}\pi + 2 - 2\log[\tfrac{1}{4}\gamma\,\Delta x\,(\omega/c_t)]\}. \tag{A4}$$

(iii) Between points lying one on the M_1 surface and the other on the M_2 surface,

$$G(n1|m2) = -(\mathrm{i}/4C_{44})H_0^{(1)}[\![(\omega/c_t)\{(x_n-x_m)^2+[\xi(n)]^2\}^{1/2}]\!] \tag{A5}$$

$$G(n2|m1) = -(\mathrm{i}/4C_{44})\{1+[\xi'(m)]^2\}^{1/2}H_0^{(1)}[\![(\omega/c_t)\{(x_n-x_m)^2+[\xi(m)]^2\}^{1/2}]\!]. \tag{A6}$$

The elements of the matrix $\Delta_a(MM)$ as defined by equation (11) are as follows.

(i) Between two points of the M_1 surface,

$$\Delta_a(n1|m1) = -[(i\,\Delta x\,\omega)/4c_t] \times [[\{-\xi'(m)(x_n - x_m) + [\xi(n) - \xi(m)]\}/\{(x_n - x_m)^2 + [\xi(n) - \xi(m)]^2\}^{1/2}]] \times H_1^{(1)}[[(\omega/c_t)\{(x_n - x_m)^2 + [\xi(n) - \xi(m)]^2\}^{1/2}]] \qquad m \neq n \tag{A7}$$

where

$$H_1^{(1)}(z) = J_1(z) + iY_1(z) \tag{A8}$$

$$\Delta_a(n1|n1) = \tfrac{1}{2} - (\Delta x/4\pi)[[\xi''(n)/\{1 + [\xi'(n)]^2\}]]. \tag{A9}$$

(ii) Between two points of the M_2 surface,

$$\Delta_a(n2|m2) = 0 \qquad m \neq n \tag{A10}$$

$$\Delta_a(n2|n2) = \tfrac{1}{2}. \tag{A11}$$

(iii) Between points lying one on the M_1 surface and the other on the M_2 surface,

$$\Delta_a(n1|m2) = [(i\,\Delta x\,\omega)/4c_t][[\xi(n)/\{(x_n - x_m)^2 + [\xi(n)]^2\}^{1/2}]] \times H_1^{(1)}[[(\omega/c_t)\{(x_n - x_m)^2 + [\xi(n)]^2\}^{1/2}]] \tag{A12}$$

$$\Delta_a(n2|m1) = -(i\,\Delta x\,\omega/4c_t)[[[-\xi'(m)(x_n - x_m) - \xi(m)]/\{(x_n - x_m)^2 + [\xi(m)]^2\}^{1/2}]] \times H_1^{(1)}[[(\omega/c_t)\{(x_n - x_m)^2 + [\xi(m)]^2\}^{1/2}]]. \tag{A13}$$

A2. The semi-infinite material (figure 1(b))

After equation (14), the matrix elements of the surface Green function $\mathbf{g}_b$ along $M_2(-R \leqslant x_1 \leqslant R, x_3 = 0)$ are

$$g_b(n2|m2) = -(i/2C_{44})H_0^{(1)}((\omega/c_t)|x_n - x_m|) \qquad n \neq m \tag{A14}$$

$$g_b(n2|n2) = -(1/2\pi C_{44})[[i\pi + 2 - 2\log\{\tfrac{1}{4}\gamma[(\Delta x\,\omega)/c_t]\}]]. \tag{A15}$$

A3. The channel (figure 1(c))

After equation (17), the matrix elements of the surface Green function $\mathbf{g}_b$ along the M_1 surface of the channel are

$$g_b(n1|m1) = -(i/4C_{44})\{1 + [\xi'(m)]^2\}^{1/2} \times (H_0^{(1)}[[(\omega/c_t)\{(x_n - x_m)^2 + [\xi(n) - \xi(m)]^2\}^{1/2}]] + H_0^{(1)}[[(\omega/c_t)\{(x_n - x_m)^2 + [\xi(n) + \xi(m)]^2\}^{1/2}]]) \qquad m \neq n \tag{A16}$$

$$g_b(n1|n1) = -(i/4C_{44})\{1+[\xi'(n)]^2\}^{1/2} \times (1-2i/\pi+(2i/\pi)\log[\tfrac{1}{4}\gamma\Delta x(\omega/c_t)\{1+[\xi'(n)]^2\}^{1/2}]+H_0^{(1)}[(2\omega/c_t)|\xi(n)|]). \tag{A17}$$

The elements of the matrix $\Delta_c(M_1M_1)$ of equation (17) are

$$\begin{aligned}\Delta_c(n1|m1) = {} & (i/4)\,\Delta x\,(\omega/c_t) \\ & \times [\{-\xi'(m)(x_n-x_m)+[\xi(n)-\xi(m)]\}/\{(x_n-x_m)^2+[\xi(n)-\xi(m)]^2\}^{1/2}] \\ & \times H_1^{(1)}[(\omega/c_t)\{(x_n-x_m)^2+[\xi(n)-\xi(m)]^2\}^{1/2}]+(i/4)\,\Delta x\,(\omega/c_t) \\ & \times [\{-\xi'(m)(x_n-x_m)-[\xi(n)+\xi(m)]\}/\{(x_n-x_m)^2+[\xi(n)+\xi(m)]^2\}^{1/2}] \\ & \times H_1^{(1)}[(\omega/c_t)\{(x_n-x_m)^2+[\xi(n)+\xi(m)]^2\}^{1/2}] \qquad n\neq m\end{aligned} \tag{A18}$$

$$\Delta_c(n1|n1) = \tfrac{1}{2}+(\Delta x/4\pi)[\xi''(n)/\{1+[\xi'(n)]^2\}]+(i/4)\,\Delta x\,(\omega/c_t)H_1^{(1)}[(2\omega/c_t)|\xi(n)|]. \tag{A19}$$

The matrix elements of $\Delta_w(M_1M_1)$ needed in equation (18) for the calculation of the Green function elements of $\mathbf{g}_w(M_1M_1)$ are

$$\Delta_w(n1|m1) = -\Delta_c(n1|m1) \qquad n\neq m \tag{A20}$$

$$\Delta_w(n1|n1) = \tfrac{1}{2}-(\Delta x/4\pi)[\xi''(n)/\{1+[\xi'(n)]^2\}]-(i/4)\,\Delta x\,(\omega/c_t)H_1^{(1)}[(2\omega/c_t)|\xi(n)|]. \tag{A21}$$

References

[1] Maradudin A A, Ryan P and McGurn A R 1988 *Phys. Rev.* B **38** 3068
[2] Djafari-Rouhani B and Maradudin A A 1990 *Solid State Commun.* **73** 173
[3] Morse P M and Feshbach H 1953 *Methods of Theoretical Physics* vol I (New York: McGraw-Hill)
[4] Inglesfield J E 1971 *J. Phys. C: Solid State Phys.* 4 L4
[5] Garcia-Moliner F and Rubio J 1969 *J. Phys. C: Solid State Phys.* **2** 1789; 1971 *Proc. R. Soc.* A **234** 257
[6] Dobrzynski L 1990 *Surf. Sci. Rep.* **11** 139
[7] Garova E A, Plessky V P, Shibanova N N and Simonian A W 1991 *Preprint*
[8] Garova E A, Kurach T N, Plessky V P and Shibanova N N 1991 *Preprint*
[9] Tran P and Maradudin A A 1992 *Phys. Rev.* B **45** 3936
[10] Macon L, Desideri J P and Sornette D 1991 *Phys. Rev.* B **44** 6755, and references therein
[11] Ling Ye, Cody G, Minyao Zhou and Ping Sheng 1992 *Phys. Rev. Lett.* **69** 3080